ARMY RESEARCH LABORATORY

# Modeling Ellipsometry for $SrTiO_3$ MBE Epitaxial Films on Si(100)

**by Daniel M. Potrepka**

**ARL-TR-5435** **January 2011**

**Approved for public release; distribution unlimited.**

## NOTICES

### Disclaimers

The findings in this report are not to be construed as an official Department of the Army position unless so designated by other authorized documents.

Citation of manufacturer's or trade names does not constitute an official endorsement or approval of the use thereof.

Destroy this report when it is no longer needed. Do not return it to the originator.

**Army Research Laboratory**
Adelphi, MD 20783-1197

**ARL-TR-5435** **January 2011**

# Modeling Ellipsometry for $SrTiO_3$ MBE Epitaxial Films on Si(100)

**Daniel M. Potrepka**
**Sensors and Electron Devices Directorate, ARL**

**Approved for public release; distribution unlimited.**

# REPORT DOCUMENTATION PAGE

***Form Approved***
***OMB No. 0704-0188***

Public reporting burden for this collection of information is estimated to average 1 hour per response, including the time for reviewing instructions, searching existing data sources, gathering and maintaining the data needed, and completing and reviewing the collection information. Send comments regarding this burden estimate or any other aspect of this collection of information, including suggestions for reducing the burden, to Department of Defense, Washington Headquarters Services, Directorate for Information Operations and Reports (0704-0188), 1215 Jefferson Davis Highway, Suite 1204, Arlington, VA 22202-4302. Respondents should be aware that notwithstanding any other provision of law, no person shall be subject to any penalty for failing to comply with a collection of information if it does not display a currently valid OMB control number.
**PLEASE DO NOT RETURN YOUR FORM TO THE ABOVE ADDRESS.**

| 1. REPORT DATE *(DD-MM-YYYY)* | 2. REPORT TYPE | 3. DATES COVERED (From - To) |
|---|---|---|
| January 2011 | Summary | May to September 2010 |

**4. TITLE AND SUBTITLE**
Modeling Ellipsometry for $SrTiO_3$ MBE Epitaxial Films on Si(100)

**5a. CONTRACT NUMBER**

**5b. GRANT NUMBER**

**5c. PROGRAM ELEMENT NUMBER**

**6. AUTHOR(S)**
Daniel M. Potrepka

**5d. PROJECT NUMBER**

**5e. TASK NUMBER**

**5f. WORK UNIT NUMBER**

**7. PERFORMING ORGANIZATION NAME(S) AND ADDRESS(ES)**
U.S. Army Research Laboratory
ATTN: RDRL-SER-L
2800 Powder Mill Road
Adelphi, MD 20783-1197

**8. PERFORMING ORGANIZATION REPORT NUMBER**
ARL-TR-5435

**9. SPONSORING/MONITORING AGENCY NAME(S) AND ADDRESS(ES)**

**10. SPONSOR/MONITOR'S ACRONYM(S)**

**11. SPONSOR/MONITOR'S REPORT NUMBER(S)**

**12. DISTRIBUTION/AVAILABILITY STATEMENT**
Approved for public release; distribution unlimited.

**13. SUPPLEMENTARY NOTES**

**14. ABSTRACT**
$SrTiO_3$ (STO) was deposited onto silicon using Molecular Beam Epitaxy (MBE). In order to characterize the sample, x-ray diffraction (XRD) measurements were made for the film, and the optical constants were obtained from ellipsometry measurements. STO XRD showed that the STO was textured with rocking curve full width at half maximum (FWHM) 0.65 $\pm$ 0.07 degrees. Optical constants were obtained from fitting of the film's ellipsometric parameters, Psi and Delta, and the thickness of the STO film was determined to be 23.6 nm. Preliminary deposition of $PbZr_{0.52}Ti_{0.48}O_3$ (PZT) showed the presence of only the 100 orientation for PZT XRD peaks.

**15. SUBJECT TERMS**
STO on Si, ellipsometry, x-ray diffraction, modeling, optical constants, thickness

| 16. SECURITY CLASSIFICATION OF: | | | 17. LIMITATION OF ABSTRACT | 18. NUMBER OF PAGES | 19a. NAME OF RESPONSIBLE PERSON |
|---|---|---|---|---|---|
| | | | | | Daniel M. Potrepka |
| a. REPORT | b. ABSTRACT | c. THIS PAGE | | | 19b. TELEPHONE NUMBER (*Include area code*) |
| UNCLASSIFIED | UNCLASSIFIED | UNCLASSIFIED | UU | 20 | (301) 394-0389 |

**Standard Form 298 (Rev. 8/98)**
**Prescribed by ANSI Std. Z39.18**

# Contents

**List of Figures** **iv**

**List of Tables** **iv**

**1. Introduction** **1**

**2. Experiment** **1**

**3. Results and Discussion** **2**

3.1 X-ray Diffraction ..... 2

3.2 Ellipsometry ..... 5

3.3 Optical Constants ..... 6

3.4 Thickness of the STO ..... 8

3.5 PZT XRD Characterization ..... 8

**4. Conclusion** **9**

**5. References** **10**

**Distribution List** **11**

## List of Figures

Figure 1. (a) XRD scan for MBE-grown STO on Si (100)—samples T0061, T0083, and T0084, and (b) same but at full intensity range to show height of Si (400) peak. ..... 2

Figure 2. STO rocking curves for (a) 200 and (b) 400 x-ray peaks of STO. ..... 4

Figure 3. Ellipsometry parameters for STO on Si (100) sample T0083 at angles of incidence 55, 60, 65, 70, and 75 degrees. ..... 5

Figure 4. Optical constants for 20 nm STO/Si deposited by MBE resemble those of a bulk STO sample (h = 4.13566733(10)×$10^{-15}$ eV*s). ..... 7

Figure 5. Oriented PZT on STO/Si sample T0061. ..... 9

## List of Tables

Table 1. X-ray diffraction peak positions for 200 and 400 STO peaks. ..... 3

Table 2. X-ray diffraction statistics for rocking curve scans of the 200 and 400 STO peaks. FWHM and $X_C$ are in degrees (2θ) ..... 5

## Acknowledgment

The author wishes to acknowledge Eric Readinger (Veeco Instruments Inc.) for preparation of the STO/Si sample, Luz Sanchez (ARL) for processing the PZT, and Ron Synowicki (J.A. Woollam Co., Inc.) for his many discussions about ellipsometer modeling.

INTENTIONALLY LEFT BLANK.

## 1. Introduction

$SrTiO_3$/silicon (STO/Si) wafers with high crystalline quality and smooth surface morphology are highly desirable for developing novel devices such as next generation dynamic random access memory and oxide field effect devices. Very high quality STO/Si epitaxial wafers are being investigated to prepare for production using the Molecular Beam Epitaxy (MBE) platform (*1*). This focus on high quality STO on Si has, in turn, stimulated interest in STO/Si as a platform for templating $PbZr_{0.52}Ti_{0.48}O_3$ (PZT) growth. It is desirable to improve PZT 100 orientation for device applications in order to maximize the d31 piezo response, thereby achieving maximum electrical response in the 100 direction in order to maximize stress orthogonal to the 100 orientation.

This work will characterize MBE-grown STO/Si through ellipsometric measurement of the STO and compare the results to those for similar measurements on bulk and thin film STO in the literature. In this work, ellipsometric measurements were made on STO/Si deposited after in situ Si procedures to clean the surface and remove native oxide, and pre-deposition of a template seed layer. The STO film is characterized by x-ray diffraction (XRD) measurements, and its thickness was obtained after modeling of the ellipsometric data. A PZT film deposited on the STO was subsequently characterized and found to be oriented in the 100 direction, ideal for PZT growth.

## 2. Experiment

Three 20 nm thick STO films, supplied by Veeco Inst. Inc., were deposited under similar conditions onto ozone-cleaned Si 100 using a Veeco GEN 10 Automated MBE system, with proprietary control of oxygen pressure (< 2.0 % deviation) and ramp rate (*2*).

I made XRD measurements for all the films using a Rigaku Ultima III diffractometer, with a CuK$\alpha$ x-ray source (tube) in the Bragg Brentano (focusing) measurement mode. A $\theta$-2$\theta$ scan was made at 20–110° using a 0.01° step width, and a 1 deg/min scan rate for 2$\theta$. Rocking curves were then measured for the 200 and 400 peaks at 0.02° step width, and a 1 deg/min scan rate, varying $\theta$ over a range of 21–25° while holding 2$\theta$ fixed at the peak maximum measured in the $\theta$-2$\theta$ scan. The full width at half maximum (FWHM) was then computed for each rocking curve.

I obtained ellipsometric parameters $\Psi$ and $\Delta$ of the STO/Si using the Woollam M200F ellipsometer. For these measurements, the angle of incidence was varied over the range of 55–75°, and the photon source provided measurements over the range of 200–1000 nm. The data was analyzed with WVase 32 software provided by the J.A. Woollam Co., Inc. in order to obtain

optical constants and a model for STO/Si. This was used to compute the thickness of the STO films.

Four layers of PZT were deposited onto a $PbTiO_3$ seed layer on the STO Sample #T0061 by MOSD spin-on method. Pyrolysis was done at 350 °C for 2 min (not strict ramp schedule), then an RTA anneal was done by ramping the temperature at 4 °C per minute to 700 $^{o}$C and holding temperature for 60 s. The PZT was then characterized by XRD. For this, a scan at 20–110° was used with a 0.01° step-width and a scan rate of 1 deg/min in 2θ.

## 3. Results and Discussion

### 3.1 X-ray Diffraction

Figure 1a shows that the strained Si 200 peak occurs for Sample T0061, and that textured STO is indicated by the presence of the 100, 200, and 400 STO peaks. For reference, figure 1b shows the height of the Si 400 peak, which is cut off at the top of figure 1a.

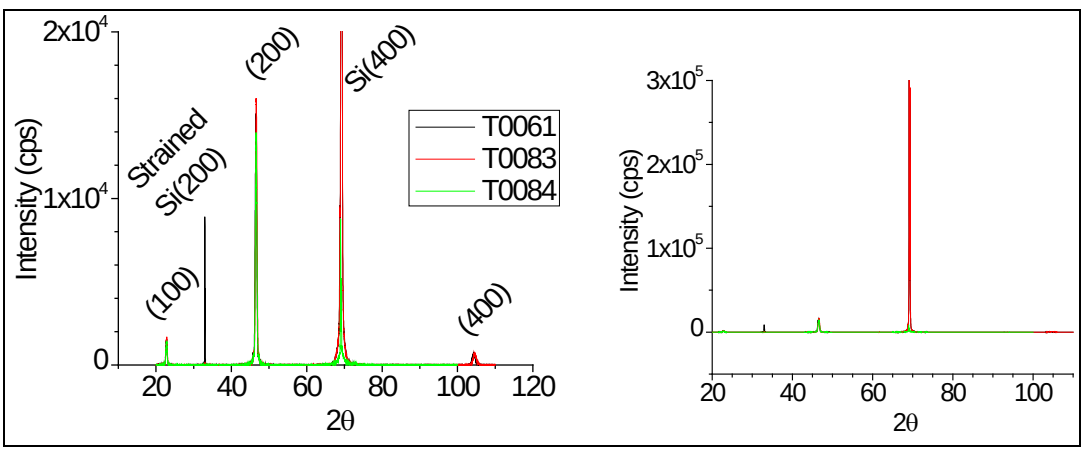


Figure 1. (a) XRD scan for MBE-grown STO on Si (100)—samples T0061, T0083, and T0084, and (b) same but at full intensity range to show height of Si (400) peak.

The positions of the 200 and 400 STO peaks are given in table 1 in degrees (2θ). Variations in position can be attributed to slight misorientation of the Si crystal from sample to sample, relative to the normal in the x-ray holder. An external alumina standard was used to verify repeatability of wafer placement in the sample holder, with repeatability of the 012, 116, and 226 $Al_2O_3$ peaks. Variations in position were verified to be $\lesssim$ 0.02 degrees over the course of 20 placements of the standard into the sample holder over a 4-month time-span around the time of the measurement. These alumina standard measurements documented the stability of the alignment of the x-ray tube, sample, sample holder, and detector as well as negligible aging effects in the x-ray tube for the duration of the measurement period.

Table 1. X-ray diffraction peak positions for 200 and 400 STO peaks.

**Theta-2Theta Scans**
**Peak Positions (degrees) obtained from Gaussian Fits and manually with cursor in JADE**

| Sample | STO(200) | STO(400) |
|---|---|---|
| T0061 | 46.52618 | 104.36396 |
| T0083 | 46.60465 | 104.5851 |
| T0084 | 46.56562 | 104.49336 |

Figures 2a and 2b show the rocking curves for the 200 and 400 STO peaks. Using equation 1, a Pearson VII fit was performed on the rocking curve XRD statistics. The peak position ($X_C$), peak area ($A$), and FWHM ($w$ in equation 1) that were generated are given in table 2, along with the dimensionless parameter $\mu$.

(a)

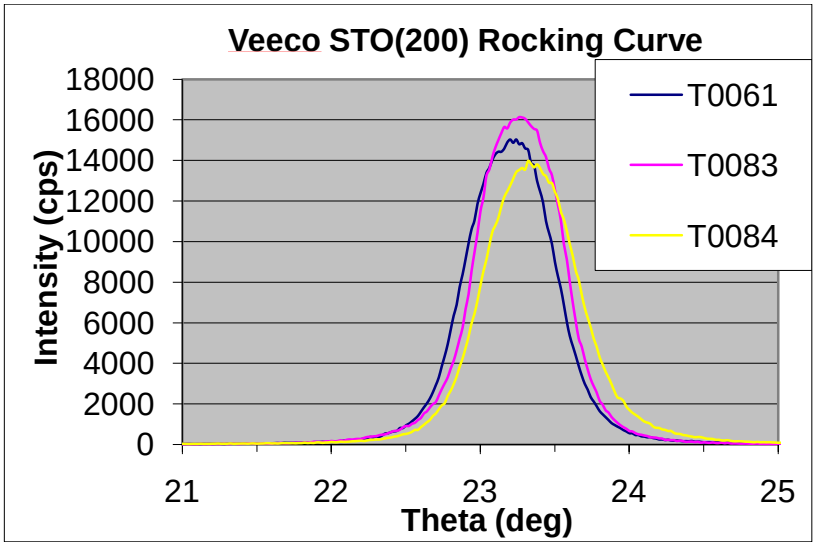


(b)

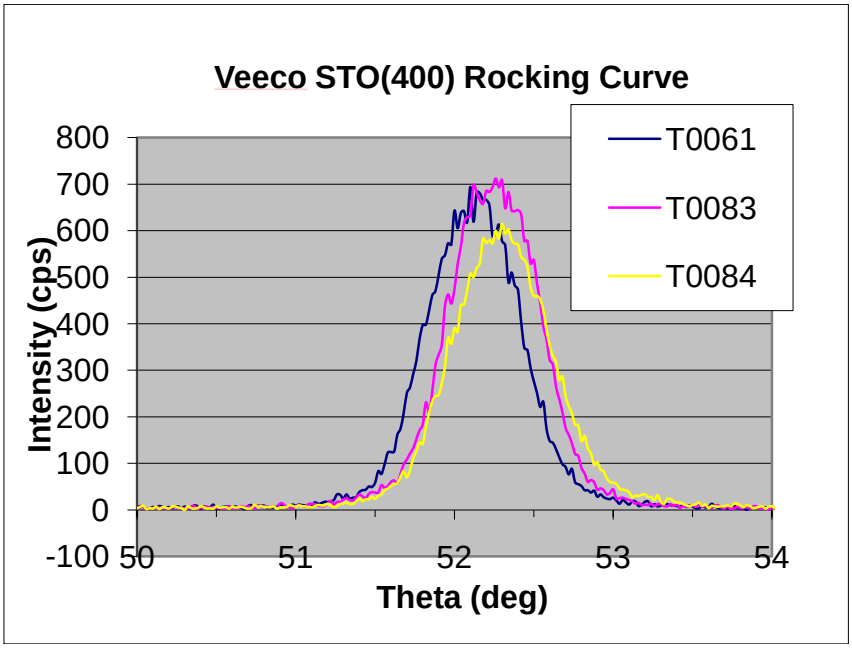


Figure 2. STO rocking curves for (a) 200 and (b) 400 x-ray peaks of STO.

$$y = A\frac{2\sqrt{\mu}e^{\left(\Gamma\left(2^{1/\mu}-1\right)\right)}}{\pi e^{\left(\Gamma(\mu-0.5)\right)}W}\left[1+4\frac{2^{1/\mu}-1}{W^2}(x-x_c)^2\right]^{-\mu} \quad (1)$$

Table 2. X-ray diffraction statistics for rocking curve scans of the 200 and 400 STO peaks. FWHM and $X_C$ are in degrees (2θ).

| Sample | FWHM(200) | *Xc*(200) | *A*(200) | *μ* (200) | FWHM(400) | *Xc*(400) | *A*(400) | *μ* (400) |
|---|---|---|---|---|---|---|---|---|
| T0061 | 0.57699 | 23.20149 | 22624.22 | 1.38862 | 0.68344 | 52.1224 | 876.0439 | 28.79689 |
| T0083 | 0.65229 | 23.26177 | 20668.58 | 169.26792 | 0.66636 | 52.24845 | 908.8244 | 170.3579 |
| T0084 | 0.70936 | 23.3839 | 19524.41 | 7.97372 | 0.71006 | 52.29615 | 839.1938 | 6.13653 |

Sample #T0061 and T0083 exhibit slightly sharper rocking curve peaks than that of Sample #T0084 as shown by their smaller FWHM, 0.67-0.68° versus 0.71°.

### 3.2 Ellipsometry

The experimental optical parameters, $\Psi$ and $\Delta$, obtained by ellipsometry measurements are shown in figure 3. These are related to the reflectance coefficients, $R_P$ and $R_S$, by

$$\tan(\Psi)\, e^{i\Delta} = \frac{R_P}{R_S} \ , \tag{2}$$

which in turn are related to the optical constants through appropriate modeling to Fresnel's equation (*3–5*).

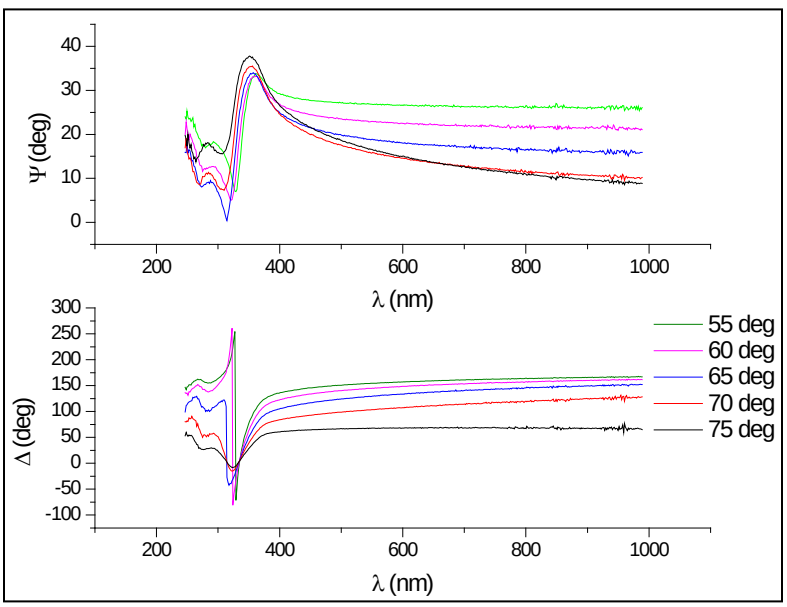


Figure 3. Ellipsometry parameters for STO on Si (100) sample T0083 at angles of incidence 55, 60, 65, 70, and 75°.

Data analysis proceeds as follows (*6*): after a sample is measured, a model is constructed to describe the sample. The model is used to calculate the predicted response from Fresnel's equations, which describe each material with thickness and optical constants. If these values are not known, an estimate is given in order to provide a preliminary calculation. The calculated

values are compared to experimental data. Any unknown material properties can then be varied to improve the match between experiment and calculation. The number of unknown properties should not exceed the amount of information contained in the experimental data. For example, a single-wavelength ellipsometer produces two data points ($\Psi$, $\Delta$), which allows a maximum of two material properties to be determined. Finding the best match between the model and the experiment is typically achieved through regression. An estimator, like the Mean Squared Error (MSE), is used to quantify the difference between curves. The unknown parameters are allowed to vary until the minimum MSE is reached. The best answer corresponds to the lowest MSE.

### 3.3 Optical Constants

The optical constants for a material will vary for different wavelengths and must be described at all wavelengths probed with the ellipsometer (*6*). A table of optical constants can be used to predict the material's response at each wavelength. However, it is not very convenient to adjust unknown optical constants on a wavelength-by-wavelength basis. It is more advantageous to use all wavelengths simultaneously. A dispersion relationship often solves this problem by describing the optical constant shape versus wavelength. The adjustable parameters of the dispersion relationship allow the overall optical constant shape to match the experimental results. Compared to fitting individual *n*, *k* values at every wavelength, this greatly reduces the number of unknown "free" parameters. For transparent materials, the index is often described using the Cauchy or Sellmeier relationship.

A point-by-point fit was made relating the optical constants to the optical parameters allowing the sample thickness to vary in order to generate the optical constants consistent with Fresnel's equation. These are plotted versus the photon energy in figure 4 ($h = 4.13566733(10)\times10^{-15}$ eV∗s). The modeling for this analysis involved solving the Fresnel equations for an adjustable parameter optical model with:

- a Cauchy layer with Urbach absorption as the starting model to represent the STO (*7*)
- the underlying Si wafer represented as a fixed model - a Si crystal 1 mm thick according to the model of (*8*).

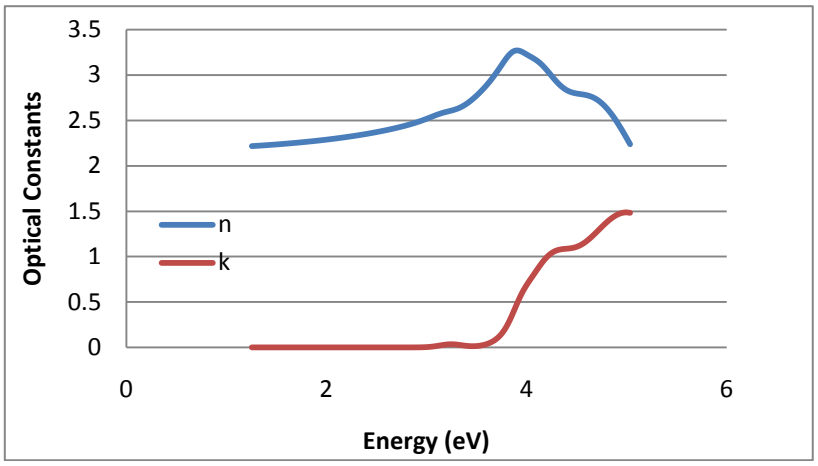


Figure 4. Optical constants for 20 nm STO/Si deposited by MBE resemble those of a bulk STO sample (h = 4.13566733(10)×$10^{-15}$ eV*s).

Four Gaussian Oscillators were used in the oscillator model for STO. The oscillators can be described by a Gaussian lineshape in $\varepsilon_2$ with a Kramers-Kronig consistent line shape for $\varepsilon_1$ (*9–11*)

$$\varepsilon_{n_Gaussian} = \varepsilon_{n1} + i\varepsilon_{n2}, \tag{3}$$

$$\varepsilon_{n2} = A_n e^{-\left(\frac{E-E_n}{\sigma}\right)^2} - A_n e^{-\left(\frac{E+E_n}{\sigma}\right)^2}, \tag{4}$$

$$\sigma = \frac{Br_n}{2\sqrt{Ln(2)}}, \tag{5}$$

$$\varepsilon_{n1} = \frac{2}{\pi} P \int_0^\infty \frac{\xi \varepsilon_{n2}(\xi)}{\xi^2 - E^2} d\xi, \tag{6}$$

where the $1/2\sqrt{\ln(2)}$ factor sets the broadening parameter, and $Br_n = FWHM$.

Comparing our optical constants (figure 4) to those reported by others (*4*, *12–14*) for single crystal STO, we find that our curves are the same except for minor local variations in magnitude. Our refractive index plot, *n*, versus energy exhibits local maxima with similar magnitudes at 4.0 eV and 4.8 eV. Our extinction coefficient plot, *k*, versus energy exhibits the same absorption onset at 3.71 eV, and turning points of approximately the same magnitude at 4.3 eV, 4.7 eV, and 4.5 eV. Van Benthem obtained direct and indirect band gap energies using linear fits to the optical absorption coefficient ($\alpha = 4\pi k/\lambda$) calculated from the ellipsometric extinction coefficient (*4*). These band-gap energies can vary depending on the range of absorption coefficients used in the linear fit (*15*). Comparing our data to that obtained by Zollner for both bulk and thin film STO (*12*), we found that unlike the films he studied, our data closely resembles that of his bulk STO plots as well as those of the van Benthem (*4*), Palik (*13*), and Trepakov (*14*) experimental groups, exhibiting similarly well-resolved structure at 3–5 eV.

### 3.4 Thickness of the STO

Thickness measurements are not independent of the optical constants (*6*). The film thickness affects the path length of light traveling through the film, but the index determines the light waves' velocity and refracted angle. Thus, both contribute to the delay between surface reflection and light traveling through the film. Both *n* and *k* must be known or determined, along with the thickness, to get the correct results from an optical measurement. The film thickness is determined by interference between light reflecting from the surface and light traveling through the film. Depending on the relative phase of the rejoining light to the surface reflection, interference can be defined as constructive or destructive. The interference involves both amplitude and phase information. The phase information from $\Delta$ is very sensitive to films down to sub-monolayer thickness. Ellipsometry is typically used for films whose thicknesses range from sub-nanometers to a few microns. Thickness measurements also require that a portion of the light travel through the entire film and return to the surface, limiting absorbing materials to thin semi-opaque layers or spectral regions with little or no absorption. The MSE (*16*) can be expressed as

$$\mathrm{MSE}(\Psi, \Delta) = \sqrt{\frac{1}{2N-M}\chi^2}, \tag{7}$$

where $N$ is the number of ($\Psi$, $\Delta$) pairs, $M$ is the number of variable parameters in the model, and $\chi = \chi(\sigma_\Psi, \sigma_\Delta)$ is the chi square, with $\sigma_\Psi$ and $\sigma_\Delta$ representing the standard deviations on the experimental $\Psi$ and $\Delta$ data points, respectively. A valid MSE is typically equal to 10 or less.

Using our final model for STO on a 1 mm thick Si substrate, we computed the thickness and MSE of the STO on (at least) 1 mm Si, and found them to be 23.592 nm and 0.9492, respectively (Sample #T0083).

The measured thickness is consistent with the predicted (~ 20 nm) thickness that is based on atom flux and growth time in the MBE, plus modeling of x-ray reflectivity measurements.

### 3.5 PZT XRD Characterization

The θ-2θ XRD plot of the PZT deposited on the STO (figure 5) confirms the desired 100 orientation with the presence of strong 100 ($I = 2\times10^5$ cps), 200 ($I = 1\times10^5$ cps), and 400 PZT peaks near 21.6, 45, and 99 deg, respectively. The small 110 and 310 PZT peaks suggest the presence of a relatively small randomly-oriented PZT component.

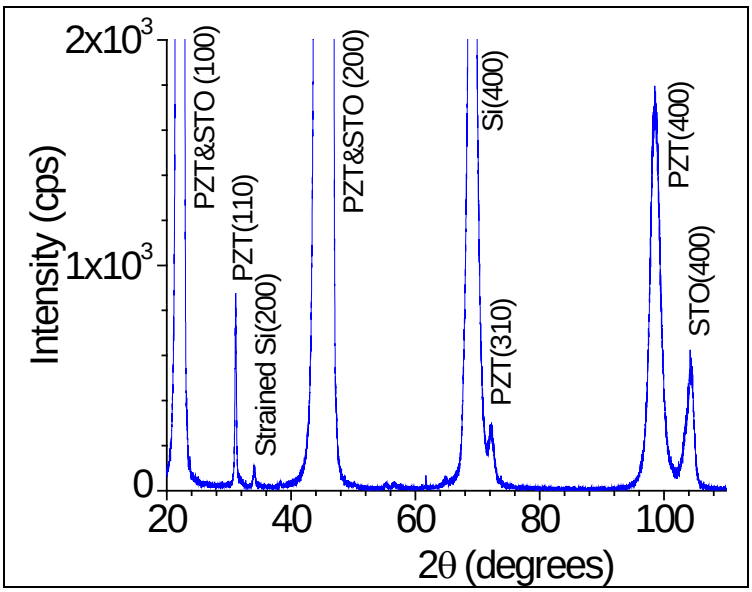


Figure 5. Oriented PZT on STO/Si sample T0061.

## 4. Conclusion

STO/Si was successfully modeled to obtain optical constants *n* and *k* consistent with values reported for single crystal STO in the literature, and superior compared to *n* and *k* reported in the literature for non-MBE films prepared on various substrates.

After generalized oscillator modeling, the thickness and MSE of the STO were computed and found to be 23.592 nm and 0.9492, respectively. The thickness is consistent with x-ray reflectivity measurements and predictions based on atom flux and growth time in the MBE. The PZT deposited on the STO is oriented in the 100 direction. A rocking curve analysis would enhance this study through quantitative characterization of the level of texture and orientation for further optimization of PZT/STO/Si film processes.

## 5. References


1. Gu, X.; Lubyshev, D.; Batzel, J.; Fastenau, J. M.; Liu, W. K.; Pelzel, R.; Magana, J. F.; Ma, Q.; Rao, V. R. Growth, Characterization, and Uniformity Analysis of 200 mm Wafer-scale $SrTiO_3$/Si. *J. Vac. Sci. Tech. B* **2010**, *28* (3), DOI: 10.1116/1.3292509, 2010.
2. Veeco film preparation – private communication from Eric Readinger, 2010.
3. *Guide to using WVASE32®*. J.A. Woollam Co. Inc., pp. 40–51, 2008.
4. van Benthem, K.; Elsässer, C.; French, R. H. Bulk Electronic Structure of $SrTiO_3$: Experiment and Theory. *J. Appl. Phys.* **2001**, *90* (12), 6156.
5. Toussaint, U. V.; Schwarz-Selinger, T.; Hopf, Christian. *AIP Conference Proceedings* 872**,** 272–279 (2006).
6. *Ellipsometry Tutorial*, http://www.jawoollam.com/ (accessed 2010).
7. *Guide to using WVASE32®*. J.A. Woollam Co. Inc., p. 250 2008.
8. Herzinger, C. M.; Johs, B.; McGahan, W. A.; Woollam, J. A.; Paulson, W. Ellipsometric Determination of Optical Constants for Silicon and Thermally Grown Silicon Dioxide via a Multi-sample, Multi-wavelength, Multi-angle Investigation. *J. Appl. Phys.* **1998**, *83* (6), 3323.
9. *Guide to using WVASE32®*. J. A. Woollam Co. Inc., p. 275. 2008.
10. De Sousa Meneses, D.; Malki, M.; Echegut, P. *J. Non-Cryst. Solids* **2006**, *351* (2), 769: Section 3.
11. Peiponen, K.-E.; Vartiainen, E. M. *Phys. Rev. B* **1991**, *44* (15), 8301.
12. Zollner, S.; Demkov, A. A.; Liu, R.; Fejes, P. L.; Gregory, R. B.; Curless, J. A.; Yu, Z.; Ramdani, J.; Droopad, R.; Tiwald, T. E.; Hilfiker, J. N.; Woollam, J. A. Optical Properties of Bulk and Thin-film $SrTiO_3$ on Si and Pt. *J. Vac. Sci. Technol. B* **2000**, *18* (4), 2242.
13. *Handbook of Optical Constants of Solids II*, edited by E. D. Palik (Academic, San Diego, CA, 1991).
14. Trepakov, V.; Dejneka, A.; Markovin, P.; Lynnyk, A.; Jastrabik, L. **2009**, *11*, 083024.
15. Matteis, L. F. *Phys. Rev. B* **1972**, *6*, 4718.
16. *Guide to using WVASE32®*. J.A. Woollam Co. Inc., p. 54, 2008.

| NO. OF COPIES | ORGANIZATION |
|---|---|
| 1 ELECT | ADMNSTR<br>DEFNS TECHL INFO CTR<br>ATTN DTIC OCP<br>8725 JOHN J KINGMAN RD STE 0944<br>FT BELVOIR VA 22060-6218 |
| 1 | OFC OF THE SECY OF DEFNS<br>ATTN ODDRE (R&AT)<br>THE PENTAGON<br>WASHINGTON DC 20301-3080 |
| 1 | US ARMY RSRCH DEV AND ENGRG CMND<br>ARMAMENT RSRCH DEV & ENGRG CTR<br>ARMAMENT ENGRG & TECHNLGY CTR<br>ATTN AMSRD AAR AEF T<br>J MATTS<br>BLDG 305<br>ABERDEEN PROVING GROUND MD 21005-5001 |
| 1 | PM TIMS, PROFILER (MMS-P)<br>AN/TMQ-52<br>ATTN B GRIFFIES<br>BUILDING 563<br>FT MONMOUTH NJ 07703 |
| 1 | US ARMY INFO SYS ENGRG CMND<br>ATTN AMSEL IE TD A RIVERA<br>FT HUACHUCA AZ 85613-5300 |
| 1 | COMMANDER<br>US ARMY RDECOM<br>ATTN AMSRD AMR<br>W C MCCORKLE<br>5400 FOWLER RD<br>REDSTONE ARSENAL AL 35898-5000 |

| NO. OF COPIES | ORGANIZATION |
|---|---|
| 1 | US GOVERNMENT PRINT OFF<br>DEPOSITORY RECEIVING SECTION<br>ATTN MAIL STOP IDAD J TATE<br>732 NORTH CAPITOL ST NW<br>WASHINGTON DC 20402 |
| 1 | US ARMY RSRCH LAB<br>ATTN RDRL CIM G T LANDFRIED<br>BLDG 4600<br>ABERDEEN PROVING GROUND MD 21005-5066 |
| 12 | US ARMY RSRCH LAB<br>ATTN IMNE ALC HRR MAIL & RECORDS MGMT<br>ATTN RDRL CIM L TECHL LIB<br>ATTN RDRL CIM P TECHL PUB<br>ATTN RDRL SER L B PIEKARSKI<br>ATTN RDRL SER L B POWER<br>ATTN RDRL SER L D POTREPKA<br>ATTN RDRL SER L G L SMITH<br>ATTN RDRL SER L J MARTIN<br>ATTN RDRL SER L J PULSKAMP<br>ATTN RDRL SER L L SANCHEZ<br>ATTN RDRL SER L R POLCAWICH<br>ATTN RDRL SER P AMIRTHARAJ<br>ADELPHI MD 20783-1197 |
| TOTAL: | 20 (18 HCS, 1 CD, 1 ELECT) |

INTENTIONALLY LEFT BLANK.